Modeling Turbulent Flow in Stirred Tanks with CFD: The Influence of the Modeling Approach, Turbulence Model and Numerical Scheme

Joelle Aubin, David F. Fletcher, Catherine Xuereb

MODELING TURBULENT FLOW IN STIRRED TANKS WITH CFD : THE INFLUENCE OF THE MODELING APPROACH, TURBULENCE MODEL AND NUMERICAL SCHEME

J. AUBIN[†‡], D.F. FLETCHER[‡] AND C. XUEREB[†*]

[†]Laboratoire de Génie Chimique UMR CNRS 5503 – INPT – ENSIACET, Toulouse, France

[‡]Department of Chemical Engineering, University of Sydney, Australia

Aubin J., Fletcher D.F. and Xuereb C., 'Modeling Turbulent Flow in Stirred Tanks with CFD: The Influence of the Modeling Approach, Turbulence Model and Numerical Scheme', *Experimental, Thermal and Fluid Science*, 28, 431-445 (2004).

Abstract

Single phase turbulent flow in a tank stirred by a down- and an up-pumping pitched blade turbine has been simulated using CFD. The effect of the modeling approach, discretization scheme and turbulence model on mean velocities, turbulent kinetic energy and global quantities, such as the power and circulation numbers, has been investigated. The results have been validated by LDV data. The stationary and time-dependent modeling approaches were found to have little effect on the turbulent flow, however the choice of the numerical scheme was found to be important, especially for the predicted turbulent kinetic energy. A first order method was found to highly underestimate LDV data compared with higher order methods. The type of the turbulence model was limited to the k-ε and RNG models due to convergence difficulties encountered with a Reynolds Stress Model (RSM) and there was found to be little effect of these models on the mean flow and turbulent kinetic energy. This latter quantity was found to be largely under predicted in the discharge region of the down-pumping impeller in comparison with LDV data. Better agreement was found for the up-pumping pitched blade turbine. Estimated power numbers were found generally to be in good agreement for the down- and up-pumping data. However, the circulation number tended to be over predicted by about 30% and 40% for the down- and up-pumping agitators, respectively.

Keywords : mixing, CFD, pitched blade turbine, up-pumping.

Introduction

During the last 10-15 years, Computational Fluid Dynamics (CFD) has become a very powerful tool in the process industry not only for the research and development of new processes but also for the understanding and optimization of existing ones. In the chemical, mineral and wastewater treatment industries, mechanically stirred tanks are widely used for either simple liquid mixing or for more complex multiphase processes, such as gas-liquid or gas-liquid solid mixing. In order to understand the complex phenomena that occur in such tanks, it is necessary to investigate the single and two phase flow fields in the vessel, as well as turbulence characteristics in turbulent applications. Advanced experimental methods, such as Laser Doppler Velocimetry (LDV) and Particle Image Velocimetry (PIV), have been shown to give detailed information on the turbulent flow field in stirred vessels for single (Aubin *et al.*, 2001; Mishra *et al*., 1998; Mavros *et al.*, 1996, 1998; Jaworski *et al*., 1996a; Ranade and Joshi, 1989; Meyers et al., 1997; Ranade *et al.*, 2001a …) and two phase (Patterson, 1991; Mishra and Joshi, 1991; Rousar and Van den Akker, 1994; Deen and Hjertager, 1999; Ranade *et al.*, 2001b) applications, providing that several experimental requirements are met. These experimental methods require that the vessel and the operating liquid are translucent in order for laser light transmission, that a transparent rectangular vessel is placed around cylindrical vessels to minimize light refraction and in the case of gas-liquid flows, that gas holdup is restricted to small quantities to avoid light scattering in LDV (Patterson, 1991) and bubble interference in PIV images (Cano, 2001). Most often in industrial situations, however, vessels are made of non-transparent materials, the operating liquids are opaque and required gassing rates are high, all of which suggest difficulties for experimental measurement of turbulent flow fields in such vessel types. For these reasons, CFD has become an important tool for the prediction of flow fields in industrial vessels to better understand flow phenomena and to optimize the processes.

The growing importance of the application of CFD to industrial problems raises a major question – are the numerical solutions physical, and correctly predicted? More and more published works on CFD in stirred vessels consist of combined experimental/numerical studies, using LDV or PIV results to validate the numerical solutions (Ranade and Joshi, 1990; Jaworski *et al.*, 1997; 1998; 2001; Sheng *et al*., 1998; Ng and Yianneskis, 2000). Most other CFD studies use previously reported experimental results in order to compare their predictions (Ranade *et al.*, 1989; Kresta and Wood, 1991; Sahu and Joshi, 1995; Ranade and Dometti, 1996; Brucato *et al.*, 1998). As a general conclusion, the authors claim that CFD satisfactorily predicts, qualitatively and quantitatively, the axial-radial mean flow patterns but under- or over-predicts the tangential velocity component and turbulent quantities, such as the turbulent kinetic energy, k, and the turbulent energy dissipation rate, ε. As CFD is based on the Navier-Stokes equations and mathematical models with simplifying assumptions, there are many sources for such discrepancies. Amongst these are the type of modeling approach employed, i.e. impeller boundary conditions (IBC), steady state or transient models, turbulence models and discretisation schemes. A few reported works compare the effect of different modeling approaches. Brucato *et al*. (1998) compare simulation results for Rushton turbines and a down-pumping axial impeller that use IBC, multiple reference frames (MFR) and sliding mesh (SM) with the k-ε turbulence model and either the hybrid upwind differencing or the QUICK discretization scheme. They showed that the results of the IBC method are very sensitive to the imposed boundary conditions themselves and satisfactory predictions rely completely on the availability and accuracy of these for a specific stirred vessel geometry. The results of the MFR method gave more accurate predictions than the IBC approach but this approach was computationally more demanding. The authors found that the SM method yielded the best agreement with experimental data for the mean flow field, although it tended to under-predict k values. The same group of authors (Micale *et al.*, 1999) carried out a similar study on dual Rushton turbines and came to the same conclusions.

The effect of discretization schemes on the simulation of flow in stirred vessels has been dealt with in very few works. Sahu and Joshi (1995) used the IBC technique to simulate the flow of down-pumping PBTs and compared three different first-order numerical schemes: the upwind scheme, the hybrid upwind scheme and the power-law scheme. They concluded that the hybrid and power-law schemes give similar results while the solution of the upwind scheme differs substantially although the latter converges more quickly than the two former schemes. No direct assessment with experimental data was made, although the authors claim that the power-law scheme is 'more robust and accurate'. Using the IBC modeling technique, Brucato *et al*. (1998) made a comparison between the solution of the hybrid upwind scheme and the third-order upwind discretization scheme QUICK. The authors concluded that the results obtained using QUICK do not differ appreciably from those using the hybrid upwind scheme except that QUICK tends to predict slightly higher recirculation rates in the top and the bottom of the tank. Roache (1998) explains that although first-order methods are computationally less expensive per grid point than higher order numerical schemes, their accuracy per overall cost is much less, so much, that the effect of the inherent numerical diffusion on solution accuracy is be devastating. Furthermore, it is interesting to note that in the policy statement of the *Journal of Fluids Engineering*, a paper will only be considered if the discretization scheme is at least second-order accurate in space (Freitas, 1993).

Several studies have focused on the effect of various turbulence models on the final numerical solution. Most commonly, a comparison between the standard k-ε and RNG k-ε models has been made. Jaworski *et al*. (1997) studied the flow produced by a Rushton turbine using a sliding mesh and reported that the type of

turbulence model did not have much effect on the mean velocities. These results showed good agreement with experimental results except for in the trailing vortex region. The turbulence quantities were found to be largely under-predicted, although better agreement with experimental data was found for the standard k-ε model than the RNG k-ε model. Later Jaworski *et al*. (2000) reported similar results to those previously discussed but for a dual Rushton turbine geometry with a tracer simulation. Without the tracer, similar results were found to those by Jaworski *et al*. (1997), with the tracer however, solution stability problems were experienced with the RNG k-ε model and the flow could not be computed.

Seeking better agreement with experimental data for turbulent flow fields than that given by the k-ε models with the isotropic assumption, and knowing that the flow (particularly in the impeller discharge) in stirred tanks has an anisotropic nature, some authors have investigated the influence of anisotropic Reynolds Stress Models (RSM) on the turbulent flow field. Armenante and Chou (1996) studied the turbulent flow produced by down-pumping single and dual six blade pitched blade turbines (PBT) using the IBC method with LDV data. They compared results employing the Algebraic Stress Model (ASM) and the standard k-ε model and reported that the results of the ASM were marginally but consistently in better agreement with the experimental data than the standard k-ε model. Bakker and Van den Akker (1994) employed the ASM using the IBC method with a first order numerical scheme to model the flows produced by a Rushton turbine, Lightnin A315 and a PBT and concluded that the results predicted by the ASM compare better with experimental data than those of the standard k-ε model. Bakker *et al*. (1996) investigated the laminar and turbulent flow patterns of a down-pumping four blade PBT using CFD. The turbulent simulations were carried out using the IBC technique with LDV data and three turbulence models (standard k-ε, RNG k-ε and RSM) were compared. The authors showed that the axial-radial velocity fields predicted by the three models gave similar results and reasonably good agreement with the experimental data, although the secondary circulation loop below the impeller was too large. Only the results of RSM showed minor differences in the top of the tank, near the baffle. Prediction of the turbulence dissipation was marginally different for the three turbulence models, but overall a large discrepancy between simulated and experimental results was found. Sheng *et al*. (1998) also predicted the flow produced by a down-pumping four blade PBT, again using IBC with LDV and PIV data, and compared the RNG k-ε model and RSM. Like the previous authors, they found good agreement with the experimental data for the mean velocity fields but the turbulence quantities were under-predicted, although it appeared that the RSM gave qualitatively better agreement. Oshinowo *et al*. (2000) studied the effect of the standard k-ε, RNG and RSM models on the tangential velocity field in a stirred tank using MFR. They found that the unphysical reverse swirl region in the upper tank predicted by simulations could be reduced by using the RNG model and were further reduced by the RSM.

Although these preceding studies are extensive in themselves, they appear to have some weaknesses with respect to the capabilities of CFD today. The majority impose IBC in order to obtain a numerical solution and even though this technique requires less computational effort, the results are very sensitive to the accuracy of the experimental data imposed at the impeller boundaries (Brucato *et al.*, 1998; Sheng *et al.*, 1998). Consequently, the use of re-scaled experimental data from a laboratory-size vessel for the simulation of larger, industrial vessels may have an influence on the numerical results (Sheng *et al.*, 1998). The papers that investigate the effect of discretization schemes generally consider first-order accurate methods that, according to Roache (1998) and Freitas (1993), are not adequate for giving accurate results. In addition to this, the authors of

the current paper believe that in order to proceed to complex multiphase CFD calculations as often found in the process industry, one first needs to obtain fully predictive results for a single phase system that have been well validated by detailed experimental data.

For the above reasons, the authors have decided to carry out a comprehensive single phase CFD study of the turbulent flow field produced by a down- and an up-pumping PBT in a dished-bottom vessel. Three modeling approaches are investigated: the traditional MFR frozen-rotor method (MFR-FR), a variant of the MFR approach that uses circumferential averaging (MFR-CA) and the sliding mesh (SM) technique. The effect of higher order numerical schemes is also assessed and compared with a first-order method. Finally, three different turbulence models have been tested using fully predictive methods. The results are validated by experimental LDV data obtained by the same group of authors.

Vessel Geometry and Grid Generation

The tank geometry employed in this work is a dish-bottomed cylindrical tank, $T = H = 0.19$m, with four equally spaced baffles ($b = T/10$) and is the same as that used for the experimental work by Aubin *et al*. (2001). A 6-blade 45° pitched blade turbine with diameter, $D = T/2$, hub diameter, $d_h = 0.2D$, and blade-width, $w_b = 0.28D$, was positioned at $C = T/3$ on a shaft that extended from the vessel base to the liquid surface. The impeller was modeled with a rotational speed, N, of 5 Hz (= 300 rpm) – corresponding to a Reynolds number of 45000 – in both the down- and up-pumping modes. The commercial mesh generator CFX-Build was used to create a structured, non-uniform multi-block grid, as shown in Figure 1, with inner and outer zones being separated by an interface in order to enable the use of sliding mesh and multiple reference frame techniques. The wide nature of the impeller blades relative to the diameter of the hub results in the overlapping of blades close to the hub. Consequently, simulation of only part of the vessel in order to decrease computational expense was not possible and therefore it was necessary to model the entire vessel geometry.

CFD Method and Model Description

CFX4 is a general purpose commercial CFD package that solves the Navier-Stokes equations using a finite volume method. In this work, CFX4.4 is used to solve the momentum, continuity and turbulence equations for fluid flow in a vessel stirred by a PBT. In this application, the impeller blades and baffles are modeled as walls with zero-thickness and a no-slip boundary condition is imposed on the vessel walls. Water at 273K is used as the operating fluid and the free liquid surface is modeled with a zero-flux and zero-stress condition applied.

Since this flow problem involves turbulent flow in a stirred tank with baffles, the resultant baffle-impeller interactions cause a periodic, time-dependent flow. This rotor-stator interaction necessitates the requirement of a modeling approach for several moving zones. Three models are available and have been used in this work: the sliding mesh model (SM) (Luo *et al.*, 1993), the frozen-rotor model (FR) and circumferential averaging model (CA). The SM model is a well known time-dependent approach that enables the periodic unsteadiness due to the relative motion of the rotating impeller and the fixed baffles to be captured. The FR model or Multiple Frames of Reference (MFR) (Luo *et al.*, 1994) technique is a steady-state approximation for problems where the distance between the impeller blades and baffles is sufficient such that the flow in the vicinity of the impeller is unaffected by the rest of the tank and can be assumed to be time-independent with respect to the impeller. The CA model is a variation of the classical FR/MFR approach whereby the connection

between the flow fields on either side of the interface is approximated for any variable by assuming that each cell sees the circumferential average of the variable in all the cells on the other side of the interface. This model is a good approximation for problems where the flow variables do not vary significantly in the tangential direction at the zone interface.

In CFD, all of the terms in each equation to be solved are discretized in space. For the discretization of the advection terms, several methods are available and the choice of the discretization method determines the accuracy of the equation solutions (since all other terms are discretized using second order methods). These schemes range from simple first order schemes to higher order schemes. Three well-known discretization schemes have been employed in this work: upwind differencing (UW), higher order upwind differencing (HUW) and quadratic upwind differencing (QUICK). When HUW or QUICK has been implemented for the three velocity components, the almost second order accurate Van Leer limiter scheme has been used for the transport equations of turbulence variables to avoid unphysical undershoots. Details of the discretization schemes are given by Hirsch (1988) and CFX4 (2001) for details and equations.

Since the operating conditions of the current problem are turbulent, the exact Navier-Stokes equations are replaced by Reynolds-averaged equations. These equations contain the Reynolds stresses which generate the need for a turbulence closure model in order to obtain a solution. It is known that the turbulence in the discharge stream of the impeller is anisotropic (Hockey and Nouri, 1996; Mishra *et al*. 1998; Aubin *et al*., 2001), which suggests that a Reynolds stress model which solves equations for the individual Reynolds stresses should be used. The differential stress model (DSM) was tested in the current study, however convergence for this particular problem proved to be extremely long and difficult with the residuals decreasing by approximately 3.0×10^{-7} per iteration and a minimum value of greater than 1.0×10^{-3}. Numerous strategies were tried to improve convergence, such as the lowering of under-relaxation factors, using the UW differencing scheme and also evoking false time stepping. However, none of these procedures improved the level of convergence and therefore further simulations using this turbulence model were abandoned. Previous work has shown that the use of first order closure models, such as the standard k-ε and Renormalization Group theory (RNG) k-ε models, which assume isotropic turbulence, give satisfactory predictions of the mean flow and hydrodynamic quantities (Bakker *et al*. (1996); Naude et al., (1998)) and qualitatively well predicted results of turbulence (Sturesson et al., 1995; Ng and Yianneskis, 2000). The standard k-ε and RNG k-ε turbulence models have therefore been used in this work. Details are given by Launder and Spalding (1972) and Fletcher *et al*. (2000). A summary of the modeling approach, discretization scheme and turbulence model employed for each simulation is given in Table 1.

Global quantities such as the power number, P_o, and the circulation number, N_c, were also calculated for each simulation case and compared with the experimental values. The power consumption was calculated using the predicted torque on the impeller blades and the equations used for the determination of both P_o and N_c are the same as given by Aubin *et al*. (2001).

CONVERGENCE CRITERIA

Simulations were typically considered converged when the mass residuals, normalized relative to the maximum circulating flow, fell below 3×10^{-4}. Further checks for convergence were made by verifying that global quantities, such as the power number, and the circulation number, were constant.

GRID REFINEMENT

A preliminary grid convergence study was carried out in order to verify that the solution is grid independent. The number of grid nodes in the x-, y- and z-directions in both the inner and outer mesh zones were systematically increased throughout the vessel such that three grids were generated – referred to as coarse, medium and fine – comprising 76,000, 155,000 and 195,000 hexahedral elements, respectively. The MFR-CA modeling approach was used with the standard k-ε turbulence model and the second order upwind discretization scheme for the three simulations. Figure 2 shows the radial profiles of turbulent kinetic energy, k, 5mm below the impeller, a zone where large transport gradients in the flow exist. It can be seen that the fine and medium grids give very similar profiles of k which differ numerically by less than 1%. The profile for the coarse grid however, is clearly different from those of the fine and medium meshes and numerically the results differ by up to 17%. Since the differences between the results for the medium and fine grid simulations are minor, the medium grid was employed for the simulations performed in this work to reduce computational requirements.

VALIDATION

The simulations described are validated using experimental LDV results obtained by the same group of authors. The experimental method for the LDV acquisitions and corresponding results come from Aubin *et al*. (2001). As the LDV data used here for validation are time-averaged, are independent of impeller-baffle position ad were taken midway between two baffles, the CFD results have been processed so that the velocity components and turbulent quantities have been averaged in the tangential direction.

Results And Discussion

DOWN-PUMPING

Comparison of Modeling Approaches

Simulated vector plots of the flow produced by the PBTD using the two MFR models and the SM technique are presented in Figures 3 (a-c). The three plots generally show similar flow patterns with a strong primary circulation loop in the lower half of the tank and a smaller secondary loop below the impeller. However, some slight differences can be noticed. In the bottom part of the vessel, the impeller jets predicted with the MFR-FR and MFR-CA techniques are discharged at less than 45° to the vertical, however with the SM approach the jet is at about 45°. As a result, the circulation loop predicted by this method is situated slightly higher up in the vessel and the secondary circulation loop is enlarged. Comparing these results with previously obtained LDV data (Aubin *et al.*, 2001), in Figure 3 (g), shows that the CFD modeling approaches predict flow patterns that are generally in good agreement, quantitatively and qualitatively, with the experimental results. Three areas, however, need special attention. In the impeller jet, the two MFR models predict the angle of discharge given by the experimental results better than the SM approach. In the lower part of the vessel, the three CFD approaches predict a secondary circulation loop which is not entirely shown by the experimental data due to inherent measurement difficulties caused by the dished bottom of the tank. The LDV results, however, show evidence of this smaller circulation loop by the conical up-flow region below the impeller and it has been shown experimentally to exist in flat bottom tanks stirred by axial flow impellers (Ranade and Joshi, 1989; Jaworski *et al.*, 1996a; Mishra *et al.*, 1998). In the upper third of the tank, although in all cases the measured and predicted

velocities are low, the flow patterns observed with the LDV are marginally different to those predicted by CFD. This may be explained by the fact that the free liquid surface in the tank is modeled with a no stress and no displacement condition applied. This means that at the surface, the velocity normal to the liquid surface, i.e. the axial velocity, is set to zero, such that the liquid level fixed. In reality this is not at all the case, as the impeller and baffles cause the liquid surface to move in all three directions.

Figures 4 (a-c) show maps of the spatial distribution of the dimensionless tangential velocity, V_θ^*, modeled by the three different techniques. The results for the three simulations give similar results. The maximum values of V_θ^* ($0.33V_{tip}$ for MFR-FR, $0.31V_{tip}$ for MFR-CA, $0.32V_{tip}$ for SM) are found in the impeller discharge and another azimuthal zone is found below the agitator, close to the vessel bottom. These results are in qualitatively good agreement with the LDV measurements of the tangential velocity field given in Figure 4 (g). The LDV results show that maximum values of V_θ^* are found in the impeller discharge, although they are twice the predicted value at $0.63V_{tip}$, and a significant swirling region below the impeller also exists. In the upper part of the tank, the three CFD models predict a significant region of liquid rotating in the opposite direction to the impeller rotation, with tangential velocities of $-0.17V_{tip}$, $-0.19V_{tip}$, and $-0.12V_{tip}$, for the MFR-FR, MFR-CA and SM models, respectively. This reverse swirl effect is much greater than that observed experimentally with the LDV measurements. As seen in Figure 4 (g), a region of liquid in reverse rotation is observed in the upper part of the tank, close to the vessel wall, but with a maximum velocity of only $-0.017V_{tip}$. The reverse swirl predicted numerically is clearly unphysical when compared with that measured experimentally and has already been reported by other numerical studies (Harris *et al.*, 1996; Oshinowo *et al.*, 2000). According to Oshinowo *et al.* (2000), this phenomenon of reverse swirl may be caused by several factors, including the location of the MFR boundary.

Dimensionless turbulent kinetic energy, k^*, maps predicted by the various modeling approaches are given in Figures 5 (a-c). For the three techniques, similar solutions have been calculated with the maximum values ($0.033V_{tip}^2$ for MFR-FR, $0.032V_{tip}^2$ for MFR-CA, $0.036V_{tip}^2$ for SM) found in the discharge region and a surrounding zone of relatively high turbulent kinetic energy. In the upper part of the vessel, the values of k^* are close to zero. Although these predictions agree qualitatively with the LDV results, quantitatively, it appears that k^* is underestimated with respect to the experimental data in the impeller discharge region. Tracing radial profiles of k^* above and below the impeller enables assessment of the results in a more local manner as shown in Figures 6 (a and b). In the upper part of the vessel at $z^* = 0.60$, it can be seen that predicted profiles have a similar form to the experimental one and there the agreement is quite good. Between $0 < r^* < 0.5R$ the three modeling approaches give very similar results but closer to the vessel wall (for $r^* > 0.5R$), the solutions are slightly different. In this area the SM technique predicts the LDV measurements quite well. Comparing the simulation results of k^* profiles in the discharge jet of the impeller ($z^* = 0.30$), indicates that the modeling approach again does not have much effect on k^* in this region of the tank. However, like the profile at $z^* = 0.60$, the time dependant solution of the SM method is slightly elevated closer to the vessel wall. This difference may be due to the fact that the SM approach takes into account the transient baffle-impeller interactions, whereas the MFR methods do not. Here in the discharge jet, there are greater differences between the predicted solutions and the experimental results than in the upper part of the tank. Not only do the forms of the graphs differ, but all modeling approaches generally under-predict the k^* values measured by LDV. This general discrepancy may be due to the fact that the impeller outflow is predicted with an isotropic turbulence model while the flow is known

to have anisotropic nature. This will be discussed further in the section investigating the effects of turbulence models.

Effect of the Discretization Scheme

Although the higher order schemes are known to be more accurate, they are often much less robust and the calculation is much slower to reach a converged solution. With this in consideration, as well as modern policies in some scientific journals, the effect of the discretization scheme on the numerical solution has been investigated. In Figures 3 (a, d, e), the velocity vectors for the reference case (FR / HUW / k-e) are compared with those predicted using the first order UW scheme and the third order QUICK scheme. Looking closely at these plots, there appears to be no effect of the discretization scheme on the mean axial or radial velocities and they predict reasonably well the experimental results shown in Figure 3 (g). Comparing the mean tangential velocity as shown in Figures 4 (a, d, e), some differences of the spatial distribution of V_θ^* can be observed. Although the maximum values determined by the three numerical schemes are located in the impeller outflow and are of similar magnitude ($0.33V_{tip}$ for HUW, $0.33V_{tip}$ for UW, $0.32V_{tip}$ for QUICK), the first order UW method under predicts (with respect to the higher order schemes) the region of swirling liquid underneath the agitator. Furthermore, QUICK predicts a small region of increased tangential velocity in the upper right area of the flow map. Comparing this with the LDV results shown in Figure 4 (g) suggests that this small area is unphysical since the experimental results show that there is liquid in reverse rotation in this region. As in the previous comparison of modeling approaches, these CFD solutions again predict the unphysical mass of reverse swirling liquid in the upper part of the tank ($-0.17V_{tip}$ for HUW, $-0.18V_{tip}$ for UW, $-0.23V_{tip}$ for QUICK), however, it appears that there is no significant effect of the discretization scheme on this phenomenon.

The type of discretization scheme employed in the simulation appears to have a significant effect on k^* in the vessel as shown in Figure 5 (a, d, e). The two higher order methods (recall that the when HUW or QUICK is used, the turbulent quantities are discretized using the second order Van Leer limiter scheme) predict a large area of maximum k^* ($0.033V_{tip}^2$ for HUW, $0.029V_{tip}^2$ for QUICK) in the discharge of the impeller, whereas the UW under predicts this region with a maximum of $0.022V_{tip}$ found only at the tip of the impeller. The experimental data in Figure 5 (g) show a similar spatial distribution of k^* with the maximum in the outflow of the agitator, although it is not of the same magnitude as the simulated values. Local profiles (in red) of k^* above and below the impeller are shown in Figures 6 (a and b), respectively. At $z^* = 0.60$, there does not appear to be an important effect of the numerical method on k^*. Furthermore, the predicted solutions agree relatively well with the experimental data. In the impeller discharge region however, the UW scheme calculates lower k^* values than both the HUW and QUICK schemes, which are very similar. As in the previous section, the numerical results, in a general way, under predict the LDV data which could be due to the anisotropic nature of the flow. However, from these results, it appears that the first order UW scheme predicts lower values of k^* than the higher order schemes in regions of high velocity gradients and anisotropic flow, such as the discharge jet. This is an important observation as it suggests that the prediction of k^* is dependent not only on the choice of turbulence model as previously suggested by studies of other authors (Armentante and Chou, 1996; Bakker *et al*., 1996; Jaworski *et al*., 1997; 2000; Sheng *et al*., 1998) but also on the differencing scheme.

Comparison of Turbulence Models

The effect of the turbulence model was investigated using only two isotropic models, the standard k-ε and the RNG models as the attempt at converging the anisotropic DSM was unsuccessful. The vector plots using the RNG model are compared with those of the reference case in Figures 3 (f) and 3 (a), respectively. In a general aspect, the two models give flow patterns that are very alike. Some small differences are noticed however in the extremities of the tank. At the bottom of the vessel, there appears to be a slight deformation of the secondary circulation loop predicted by the RNG model, that is not observed with the standard k-ε model, where it appears that the mean radial and axial velocities are close to zero. In the top of the tank, close to the liquid surface, the mean radial and axial velocities are slightly higher with the RNG model than for the reference case. This slight discrepancy could be due to the fact that the predicted tangential velocity in this upper region is relatively high and the RNG model has been found to be preferred for modeling highly swirling flows (Jaworski *et al*., 1996b).

The mean tangential velocity maps are shown in Figures 4 (a and f). As for the previously described simulations, the majority of the upper part of the tank is in a reverse swirling motion with speeds of $-0.17V_{tip}$ for the standard k-ε model and $-0.22V_{tip}$ for the RNG model, with no significant differences. This is different to the results of Oshinowo *et al*. (2000) who found that the reverse swirl region predicted using the k-ε model was reduced when the RNG model was employed, and further reduced when using the RSM. However, the Reynolds number is somewhat larger in the present study, which may explain the difference in findings. In the impeller discharge, a strong tangential flow is observed in both cases ($0.33V_{tip}$ for the standard k-ε model and $0.30V_{tip}$ for the RNG model). Below the impeller however, the RNG model predicts a slightly larger swirling region than the k-ε model which corresponds well with the vector plots.

Figures 5 (a and f) compare the turbulent kinetic energy distribution in the tank using the k-ε and RNG models, respectively. The maximum value predicted by the RNG model of $0.023V_{tip}^2$ is less than that obtained by the reference case ($0.033V_{tip}^2$), and its spatial distribution is also smaller. These results generally agree in a qualitative manner with the experimental maps in the sense that they predict maximum values in the impeller discharge. In a more local manner, Figure 6 compares the results of the two models (in green) with the LDV data. In the upper part of the vessel, both the k^* profiles predicted by the two models differ slightly in the outer half of the tank and here the RNG model is in better agreement with the experimental results. Greater differences are observed in the k^* profiles at $z^* = 0.30$ in the impeller discharge. The RNG model predicts lower levels of k^* than the standard model throughout the radius of the vessel, suggesting that the results given by the standard model are in 'closer' agreement with the experimental data. However, these data are generally under predicted by both turbulence models. As described in the introduction, this discrepancy is a common result when comparing experimental data with simulated results using the standard k-ε and RNG models. Several experimental studies have shown that turbulence in stirred vessels is generally anisotropic, especially in the impeller discharge jet (Hockey and Nouri, 1996; Mishra *et al.*, 1998; Aubin *et al.*, 2001). However, for computational ease, the turbulence models employed in the current numerical simulations are RANS based and assume isotropy, which are simplifying assumptions with respect to reality. This simplified approach to turbulence modeling may explain the significant discrepancy between the anisotropic k^* field given by LDV and predicted results. In addition to this, some authors have also mentioned that experimental measurements in the impeller inflow and outflow may contain 'pseudo-turbulence' due to the periodic high frequency fluctuations produced by the rotating impeller (Wu and Patterson, 1989; Bakker and Van den Akker, 1994; Jaworski *et al.*,

2001). Such periodic fluctuations may be the cause of increased measured fluctuations around the impeller but may have no effect near the baffle region. Other authors, however, have found that the removal of the periodic component does not significantly effect the calculation of turbulence quantities (Kresta and Wood, 1993; Sharp and Adrian, 2001).

UP-PUMPING

Having analyzed the effect of modeling approaches, discretization schemes and turbulence models on the flow produced by a down-pumping pitched blade turbine, it did not seem necessary to carry out an identical investigation for the pitched blade turbine in the up-pumping mode. Considering the results obtained in the down-pumping study, as well as computational expense, the HUW numerical scheme and the standard k-ε turbulence model were chosen and the two MFR techniques were employed for the up-pumping simulations.

Figure 7 compares the mean radial-axial velocity vectors of the two simulated cases using the MFR-FR and MFR-CA approaches with those obtained using LDV. As observed in the down-pumping case, the two MFR modeling techniques result in very similar flow patterns. Only a slight difference can be observed in the upper tank, close to the shaft where the MFR-CA approach predicts marginally smaller vectors than the MFR-FR model. This is difficult to explain since the difference in these two models is at the boundary between the inner and outer zones of the tank (see Figure 1). With respect to the experimental data, the CFD results predict the mean flow patterns and velocity magnitudes reasonably well. Looking more closely at the position of the circulation loop centers, both models agree well with the position of the experimental upper loops, however, for the lower circulation loops are estimated to be slightly higher than measured with the LDV. This could be perhaps due to the steady-state assumption applied for these calculations.

The mean tangential velocity maps obtain with the two MFR models and the LDV are shown in Figures 8 (a-c), respectively. Comparing the two predicted flow patterns, it is seen that the maximum value of V_θ^* is found in the impeller discharge region with values that are similar to the down-pumping case ($0.32V_{tip}$ for MFR-FR and $0.30V_{tip}$ for MFR-CA). Like for the down-pumping case, the bulk of the liquid in the upper part of the tank is in reverse rotation with respect to the impeller, with comparable velocities ($-0.17V_{tip}$ for MFR-FR and $-0.18V_{tip}$ for MFR-CA). In addition to this, a second region of reverse swirling liquid is observed beneath the agitator. Comparing these predictions with the LDV data suggests that the simulated results are unphysical. The LDV data show the presence of a small region of swirling liquid under the impeller but turning in the same direction as the impeller rotation. Furthermore, close to the shaft in the upper part of the tank, there is evidence of a positive tangential motion. The only reverse swirling liquid has been measured in a small region in the top of the tank with a minimal velocity ($-0.015V_{tip}$).

Dimensionless turbulent kinetic energy maps are shown in Figure 9. The distribution and magnitude of k^* predicted by the two different modeling approaches are very similar and agree reasonably well with the LDV data. Considering the local profiles of k^* above and below the impeller, as shown in Figure 10, it can be seen that the two models produce similar results. In the impeller discharge ($z^* = 0.45$), where flow is generally anisotropic, and below the impeller ($z^* = 0.30$), the predicted results are in a comparable range with the LDV data and generally show better agreement than for the down-pumping case. Aubin *et al*. (2001) showed that the PBT in up-pumping mode produced smaller velocity fluctuations in the impeller discharge than for the down-pumping

mode. Also, the flow was found to be slightly more isotropic with the up-pumping impeller. This explains the better agreement of the up-pumping calculations with LDV data than the down-pumping ones.

POWER AND CIRCULATION NUMBERS

In order to compare the different CFD modeling approaches in a more global manner, the power and circulation numbers for each simulation have been calculated and are presented in Table 2. For the down-pumping case, it can be seen that the two MFR models give very similar P_o values, whereas the SM approach predicts a slightly higher value. Compared with the experimentally measured power, these predicted P_o are just outside the error bars and are considered to be in good agreement. The type of discretisation scheme chosen appears to have a more important effect on P_o. As expected, the first order UW scheme under predicts power consumption which can be attributed to numerical diffusion. More interestingly, the QUICK scheme further under predicts P_o. Whilst convergence was acceptable, the QUICK scheme proved to much more difficult to converge due to the lower diagonal dominance of the scheme, which may have affected calculation of torque and thus P_o. Finally, the RNG turbulence model predicts a similar P_o value to the standard model, which compares well with the experimental values. For the up-pumping case, the two models predict comparable values, however, they tend to under predict the experimental P_o by approximately 10%.

The numerically determined circulation numbers for the down-pumping mode are calculated via the mean axial velocity field. Overall, there appears to be little effect of the modeling approach or the turbulence model used on this quantity. Small differences in N_c values are observed for the different discretization schemes. Comparing these numerical results with the LDV data, shows that the CFD models generally slightly over predict by about 30% the experimental data. Only the UW and QUICK schemes predict values closer to LDV value. Although it seems correct that QUICK best predicts N_c, as it is a third order scheme, it would have been expected that the HUW method results in better agreement than the UW scheme, which is not the case. As for the down-pumping configuration, calculations in the up-pumping mode also tend to over predict the circulation number measured using LDV by about 40%.

Conclusion

CFD simulations of the flow produced in a vessel stirred by an up- and a down-pumping PBT have been carried out. The investigation has focussed on the effect of three different modeling parameters (modeling approach, discretization scheme and turbulence model) on the numerical solution and these results are validated with experimental LDV data.

The choice of modeling approach, the Multiple Reference Frame (MRF) or sliding mesh (SM), has shown to only slightly affect the mean radial and axial flow patterns in the impeller discharge region, in the rest of the tank they are comparable. Overall, the results using both MFR methods are in very good agreement with the LDV data. Although poor agreement of the numerical results with LDV data was found for the mean tangential velocity, there did not appear to be a direct effect of the modeling approach on this variable. The effect of the modeling technique on k^*, was found to be slight, although values predicted by SM in the outer part of the vessel were marginally greater. Generally, the three modeling approaches were found to under predict k^*.

The type of discretization scheme was found to have no effect on the mean radial and axial velocities in the vessel, nor on the large reverse swirling region in the upper part of the tank. The first order UW method,

however, was shown to under predict a small swirling region below the impeller. Furthermore, the UW scheme also was found to significantly under predict the distribution and magnitude of k^* with respect to the higher order methods. Although all three numerical schemes have the tendency to under predict k^*, it is important to note that the first order scheme further under estimates this variable. The type of discretization scheme is therefore important for the simulation of turbulent flows and the choice could be detrimental in the simulation of multiphase flows, such as gas-liquid mixing where k^* influences bubble break-up.

The two RANS turbulence models with the isotropic assumption were found to have no significant effects on the mean radial and axial velocity fields, or on the reverse tangential motion in the upper tank unlike for Oshinowo *et a*l. (2000). The difference in the effect of the standard k-ε and RNG models on k^* itself was found to be small, and k^* values were generally under predicted, especially in the discharge jet of the impeller where flow is highly anisotropic. Although an anisotropic RSM model appears to be the simplest solution for better predicting k^*, the results given by other authors show that there is no considerable improvement on the prediction of k^* (Armenante and Chou, 1996; Bakker and Van den Akker, 1994; Bakker *et al.*, 1996; Sheng *et al.*, 1998). Consulting the published work, it appears that only Large Eddy Simulations (LES) have predicted kinetic energy levels that are in accordance with experimental data (Dersken and Van den Akker, 1999; Dersken, 2001). This suggests that such discrepancies in the prediction of turbulent quantities may arise from Reynolds averaging. The discrepancies between the predicted and measured turbulence quantities is a very important issue that must be resolved. Until one can correctly predict such quantities in a single phase flow, it will be difficult to correctly simulate complex multiphase flows, such as gas-liquid, solid-liquid, gas-solid-liquid, where turbulence plays an important role.

For the up-pumping PBT, the mean radial and axial velocities were found to be in good agreement with the LDV results. The tangential component, however, was found to be in reverse rotation in the bulk of both the upper and lower vessel. This is contradictory to the LDV data. Predicted values of k^* were found to be in closer agreement with the experimental data than for the down-pumping case, due to the lesser anisotropic nature of the up-pumping flow.

The predicted power number of the PBTD was found to be in generally good agreement with the experimental data, and although the CFD models correctly calculated a higher power number for the up-pumping configuration, these values were slightly under predicted by about 10%. For both the down- and up-pumping modes, the circulation number is overestimated by about 30% and 40%, respectively.

Nomenclature

b	Baffle width, m
C	Impeller clearance, m
d_h	Hub diameter, m
D	Impeller diameter, m
ε	Turbulent energy dissipation rate, m^2s^{-3}
H	Vessel height, m
k	Turbulent kinetic energy, m^2s^{-2}
k^*	Dimensionless turbulent kinetic energy, -
N	Impeller speed, s^{-1}
N_c	Circulation number, -
T	Vessel diameter, m
P_o	Power number, -
V_r^*, V_z^*, V_θ^*	Dimensionless radial, axial and tangential velocity, -
w_b	Impeller blade width, m
x, y, z	Cartesian co-ordinates

References

Armenante P.M. and C-C. Chou, 'Velocity Profiles in a Baffled Vessel with Single or Double Pitched-Blade Turbines', *AIChE J.*, **42**, 1, 42-54 (1996).

Aubin J., P. Mavros, D.F. Fletcher, J. Bertrand and C. Xuereb, 'Effect of Axial Agitator Configuration (Up-Pumping, Down-Pumping, Reverse Rotation) on Flow Patterns Generated in Stirred Vessels', Accepted for publication in *Trans IChemE* (2001).

Bakker A. and H.E.A.Van den Akker, 'Single-Phase Flow in Stirred Reactors', *Trans IChemE*, **72** A, 583-593 (1994).

Bakker A., K.J. Meyers, R.W. Ward and C.K. Lee, 'The Laminar and Turbulent Flow Pattern of a Pitched Blade Turbine', *Trans IChemE*, **74** A, 485-491 (1996).

Brucato A., M. Ciofalo, F. Grisafi and G. Micale, 'Numerical Prediction of Flow Fields in Baffles Stirred Vessels : A Comparison of Alternative Modelling Approaches', *Chem. Eng. Sci.*, **53**, 21, 3653-3684 (1998).

CFX, *CFX4.4 Solver Manual*, CFX International, AEA Technology, Didcot, Oxon, UK (2001).

Dersken J., 'Assessment of Large Eddy Simulations for Agitated Flows', *Proc. 4th Inter. Symp. Indust. Mixing – ISMIP4*, 14-16 May, Toulouse France (2001).

Dersken, J. and H.E.A. Van den Akker, 'Large Eddy Simulations on the Flow Driven by a Rushton Turbine', *AIChE J.*, **45**, 2, 209-221 (1999).

Fletcher D.F., B.S. Haynes, F.C. Christo and S.D. Joseph, 'A CFD Based Combustion Model of an Entrained Flow Biomass Gasifier', Appl. Math. Modelling, **24** (3), 165-182 (2000).

Freitas C.J., 'Editorial Policy Statement on the Control of Numerical Accuracy', *ASME J. Fluids Eng.*, **115**, 2, 339 (1993).

Harris C.K., D. Roekaerts, and F.J.J. Rosendal, 'Computational Fluid Dynamics for Chemical Reactor Engineering', *Chem. Eng. Sci.*, **51**, 10, 1569-1594 (1996).

Hirsch C., *Numerical Computation of Internal and External Flows. Volume 1: Fundamentals of Numerical Discretisation*, John Wiley & Sons Ltd., UK (1998).

Hockey R.M. and J.M. Nouri, 'Turbulent Flow in a Baffled Vessel Stirred by a 60° Pitched Blade Impeller', *Chem. Eng. Sci*., **51**, 19, 4405-4421 (1996).

Jaworski Z., A.W. Nienow and K.N. Dyster, 'An LDA Study of the Turbulent Flow Field in a Baffled Vessel Agitated by an Axial, Down-pumping Hydrofoil Impeller', *Can. J.Chem. Eng.*,**74**, 3-15 (1996a).

Jaworski Z., M.L. Wyszynski, R.S. Badham, K.N. Dyster, I.P.T Moore, A.W. Nienow and J. McKemmie, 'Sliding Mesh Simulation of Transitional, Non-Newtonian Flow in a Baffled Stirred Tank', *Notes on Numer. Fluid Mech.*, **53**, 109-115 (1996b).

Jaworski Z., K.N. Dyster, I.P.T. Moore, A.W. Nienow and M.L. Wyszynski, 'The Use of Angle Resolved LDA Data to Compare Two different Turbulence Models Applied to Sliding Mesh CFD Flow Simulations in a Stirred Tank', *Récents Progès en Génie des Procédés*, **11**, 51, 187-194 (1997).

Jaworski Z., W. Buljalski, N. Otomo and A.W. Nienow, 'CFD Study of Homogenisation with Dual Rushton Turbines – Comparison with Experimental Results', *Trans IChemE*, **78** A, 327-333 (2000).

Jaworski Z., M.L. Wyszynski, K.L. Dyster, V.P. Mishra and A.W. Nienow, 'A Study of an Up- and a Down-Pumping Wide-Blade Hydrofoil Impeller: Part II. CFD Analysis.', *Can. J. Chem. Eng.*, **76**, 866-876 (1998).

Jaworski Z., K.N. Dyster and A.W. Nienow, 'The Effect of Size, Location and Pumping Direction of Pitched Blade Turbine Impellers on Flow Patterns : LDA Measurements and CFD Predictions', *Proc. 4th Inter. Symp. Indust. Mixing - ISMIP4*, 14-16 May, Toulouse France (2001).

Kresta S.M. and P.E. Wood, 'Prediction of the Three-Dimensional Turbulent Flow in Stirred Tanks', *AIChE J.*, **37**, 3, 448-459 (1991).

Kresta S.M. and P.E. Wood, 'The Flow Field Produced by a Pitched Blade Turbine : Characterisation of the Turbulence and Estimation of the Dissipation Rate', *Chem. Eng. Sci.*, **48**, 1761-1773 (1993).

Launder B.E. and D.B. Spalding, *Mathematical Models of Turbulence*, Academic Press, London (1972).

Luo J.Y., A.D. Gosman, R.I. Issa, J.C. Middleton and M.K. Fitzgerald, 'Full Flow Field Computation of Mixing in Baffled Stirred Vessels', *Trans IChemE*, **71** A, 342-344 (1993).

Luo J.Y., R.I. Issa and A.D. Gosman 'Prediction of Impeller-induced Flows in Mixing Vessels using Multiple Frames of Reference', *8th European Conf. on Mixing, Cambridge*, Vol. 138, *IChemE Symposium*, 549 (1994).

Mavros P., C. Xuereb and J. Bertrand, 'Determination of 3-D Flow Fields in Agitated Vessels by Laser Doppler Velocimetry: Effect of Impeller Type and Liquid Viscosity on Liquid Flow Patterns', *Trans IChemE*, **74** A, 658-668 (1996).

Mavros P., C. Xuereb and J. Bertrand, 'Determination of 3-D Flow Fields in Agitated Vessels by Laser Doppler Velocimetry : Use and Interpretation of RMS Velocities', *Trans IChemE*, **74** A, 223-233 (1998).

Meyers K.J., R.W. Ward and A. Bakker, 'A Digital Particle Velocimetry Investigation of Flow Field Instabilities of Axial Flow Impellers', *J. Fluids Eng.*, 119, 623-631 (1997).

Mishra V.P., K.N. Dyster, Z. Jaworski, A.W. Nienow, and J. McKemmie, 'A Study of an Up- and a Down-Pumping Wide Blade Hydrofoil Impeller : Part I. LDA Measurements', *Can. J. Chem. Eng.*, **76**, 577-588 (1998).

Ng K. and M. Yianneskis, 'Observations on the Distribution of Energy Dissipation in Stirred Vessels', *Trans IChemE*, **78**, A, 334-341 (2000).

Oshinowo L., Z. Jaworski, K.N. Dyster, E. Marshall and A.W. Nienow, 'Predicting the Tangential Velocity Field in Stirred Tanks Using the Multiple Reference Frames (MRF) Model with Validation by LDA Measurements', *Proc. 10th Europ. Conf. Mixing*, Delft, 281-288 (2000).

Patterson G.K., 'Measurements and Modelling of Flow in Gas Sparged, Agitated *Vessels' Proc. 7th Europ. Conf. Mixing*, Brugges, 209-215 (1991).

Ranade V.V. and S.M.S. Dometti, 'Computational Snapshot of Flow Generated by Axial Flow Impellers in Baffled Stirred Vessels', *Trans IChemE*, **74** A, 476-484 (1996).

Ranade V.V. and J.B. Joshi J.B., 'Flow Generated by Pitched Blade Turbines I : Measurements using Laser Doppler Anemometer', *Chem. Eng. Comm.*, **81**, 197-224 (1989).

Ranade V.V., J.B. Joshi and A.G. Marathe, 'Flow Generated by Pitched Blade Turbines II : Simulations Using k-ε Model', *Chem. Eng. Comm.*, **81**, 225-248 (1989).

Ranade V.V. and J.B. Joshi, 'Flow Generated by a Disc Turbine : Part II. Mathematical Modelling and Comparison with Experimental Data, *Trans IChemE*, **68** A, 34-50 (1990).

Ranade V.V., M. Perrard, N. Le Sauze, C. Xuereb and J. Bertrand, 'Trailing Vortices of Rushton Turbine: PIV Measurements and CFD Simulations with Snapshot Approach, *Trans IChemE*, **79** A, 3-12 (2001a).

Ranade V.V., M. Perrard, N. Le Sauze, C. Xuereb and J. Bertrand, 'Influence of Gas Flow Rate on Structure of Trailing Vortices of Rushton Turbine : PIV Measurements and CFD Simulations', *Proc. 4th Inter. Symp. Indust. Mixing - ISMIP4*, 14-16 May, Toulouse France (2001b).

Rhie C.M. and W.L. Chow W.L., 'Numerical Study of the Turbulent Flow Past an Airfoil with Trailing Edge Separation', *AIAAJ*, **21**, 1527-1532 (1983).

Roache P.J., *Verification and Validation in Computational Science and Engineering*, Hermosa Publishers, New Mexico (1998).

Sahu A.K. and J.B. Joshi, 'Simulation of Flow in Stirred Vessels with Axial Flow Impellers : Effects of Various Numerical Schemes and Turbulence Model Parameters', *Ind. Eng. Chem. Res.*, **34**, 626-639 (1995).

Sharp K.V. and R.J. Adrian, 'PIV Study of Small-Scale Flow Structure Around a Rushton Turbine', *AIChE J.*, **47**, 4, 766-778 (2001).

Sheng J., H. Meng and R.O. Fox, 'Validation of CFD Simulations of a Stirred Tank Using Particle Image Velocity Data', *Can. J. Chem. Eng.*, **76**, 611-625 (1998).

Sturesson C., H. Theliander, and A. Rasmuson, 'An Experimental (LDA) and Numerical Study of the Turbulent Flow Behaviour in the Near Wall and Bottom Regions in an Axially Stirred Vessel', *AIChE Symp. Series (305)*, **91**, 102-114 (1995).

Wu H. and G.K. Patterson, 'Laser-Doppler Measurements of Turbulent Flow Parameters in a Stirred Mixer', *Chem. Eng. Sci.*, **44**, 2207-2221 (1989).

Table 1 : Operating and modeling conditions for each simulation.

Case Name	Impeller Pumping Direction	Modeling Approach	Discretization Scheme	Turbulence Model
FR / HUW / k-e	DOWN	FR	HUW	*k-ε*
CA / HUW / k-e	DOWN	CA	HUW	*k-ε*
SM / HUW / k-e	DOWN	SM	HUW	*k-ε*
FR / UW / k-e	DOWN	FR	UW	*k-ε*
FR / QUICK / k-e	DOWN	FR	QUICK	*k-ε*
FR / HUW / RNG	DOWN	FR	HUW	RNG
FR / HUW / k-e / UP	UP	FR	HUW	*k-ε*
CA / HUW / k-e / UP	UP	CA	HUW	*k-ε*

Table 2 : Comparison of predicted and measured power and circulation numbers.

	P_o	N_c
FR / HUW / k-e	1.83	1.16
CA / HUW / k-e	1.84	1.19
SM / HUW / k-e	1.99	1.20
FR / UW / k-e	1.77	1.09
FR / QUICK / k-e	1.62	0.98
FR / HUW / RNG	1.87	1.26
LDV - PBTD (Aubin *et al.*, (2001a))	**1.93±0.05**	**0.91±3%**
FR / HUW / k-e / UP	2.34	1.77
CA / HUW / k-e / UP	2.32	1.86
LDV - PBTU (Aubin *et al.*, (2001a))	**2.58±0.04**	**1.27±3%**

Figure 1 : Multi-block structured grid for the 6-blade 45° pitched blade turbine.

Figure 2 : Grid convergence testing. Effect of grid size on turbulent kinetic energy profiles ($z^* = 0.30$).

Figure 3 : Dimensionless radial-axial vector plots for the PBTD.

Figure 4 : Dimensionless tangential velocity, V_θ^*, maps for the PBTD.

Figure 5 : Dimensionless turbulent kinetic energy, k^*, maps for the PBTD.

Figure 6 : Comparison of modeling approaches, discretization schemes and turbulence models : Profiles of k^* above and below the agitator ($z^*=0.3$ and $z^*=0.6$) for the PBTD.

Figure 7 : Dimensionless radial-axial vector plots for the PBTU.

Figure 8 : Dimensionless tangential velocity, V_θ^*, maps for the PBTU.

Figure 9 : Dimensionless turbulent kinetic energy, k^*, maps for the PBTU.

Figure 10 : Comparison of modeling approaches : Profiles of k^* above and below the agitator ($z^*=0.3$ and $z^*=0.45$) for the PBTU.

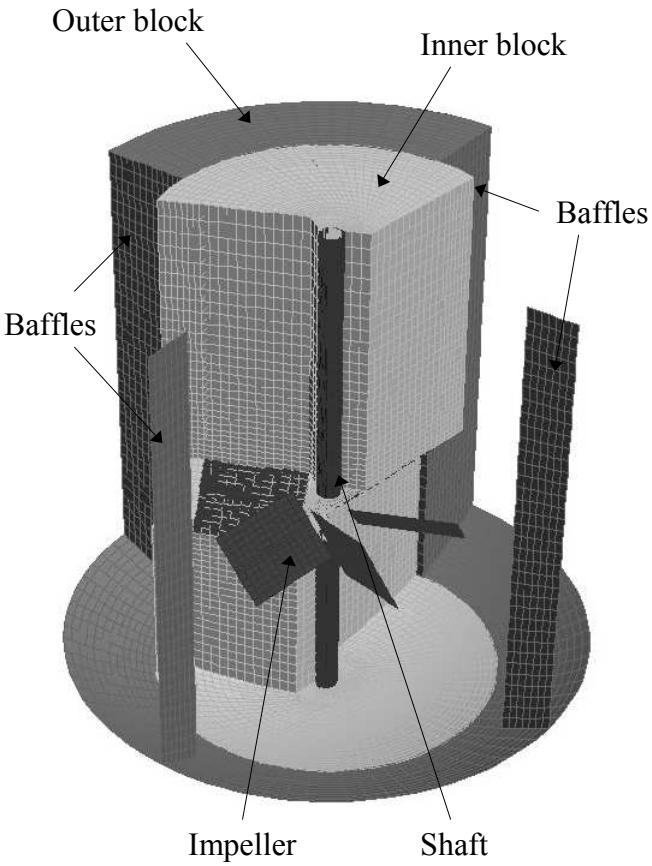

Figure 1

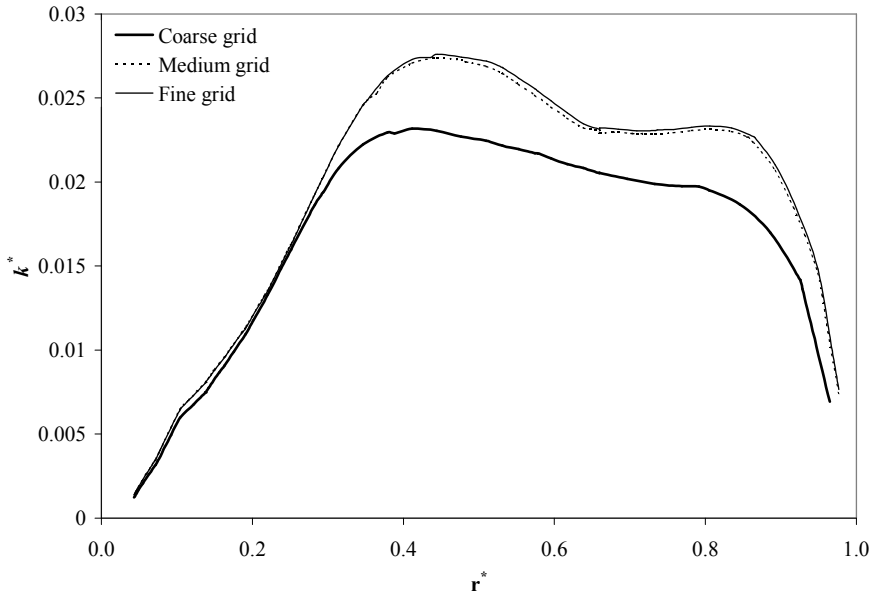
Coarse grid
Medium grid
Fine grid
0.03
0.025
0.02
0.015
0.01
0.005
0
0.0
0.2
0.4
0.6
0.8
1.0
k*
r*

Figure 2

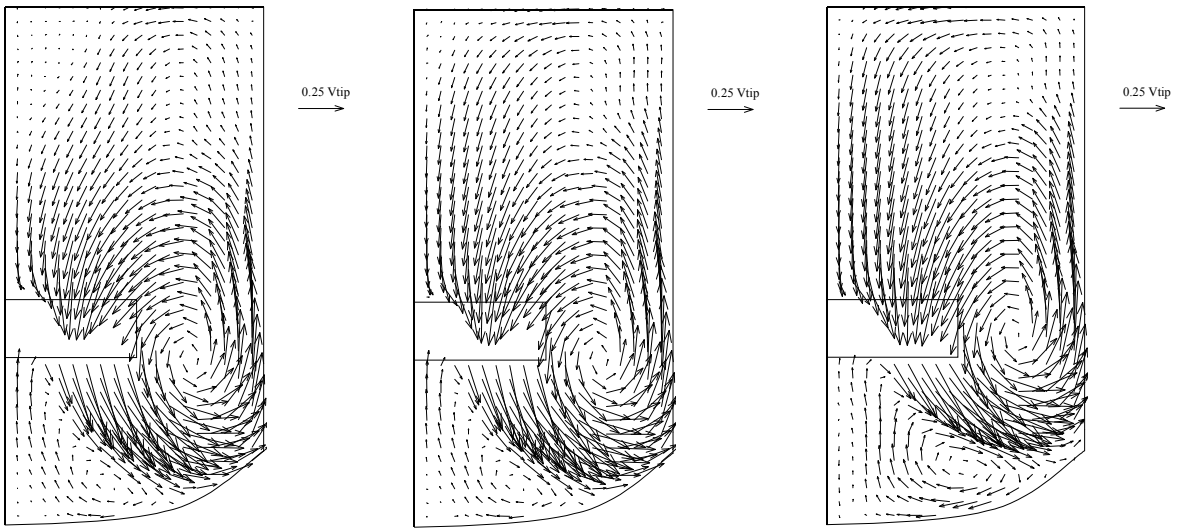

(a) FR / HUW / k-e (b) CA / HUW / k-e (c) SM / HUW / k-e

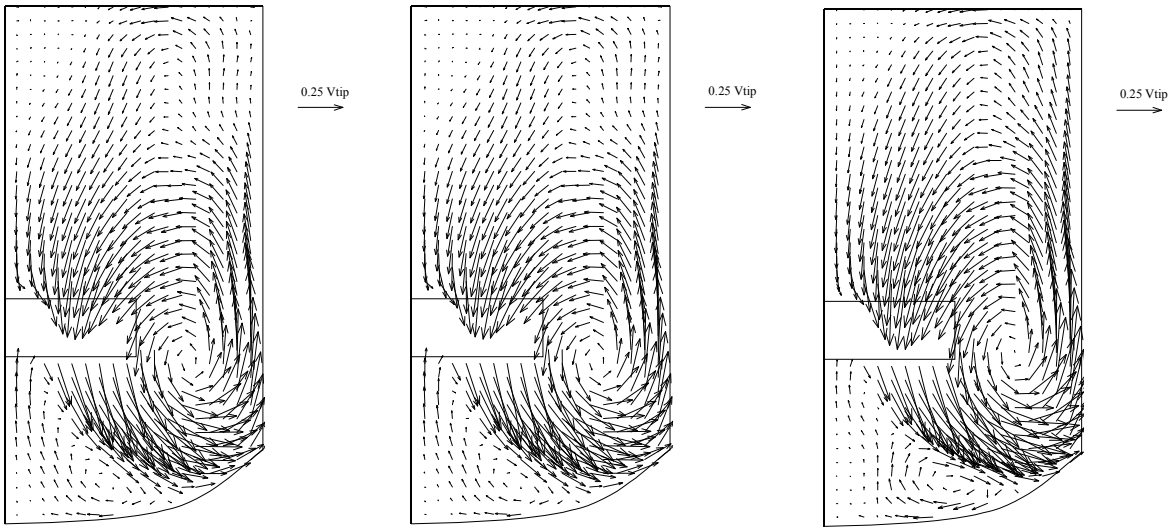

(d) FR / UW / k-e (e) FR / QDS / k-e (f) FR / HUW / RNG

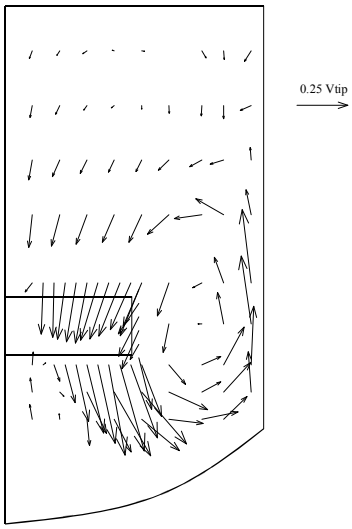

(g) LDV (Aubin *et al*., 2001)

Figure 3

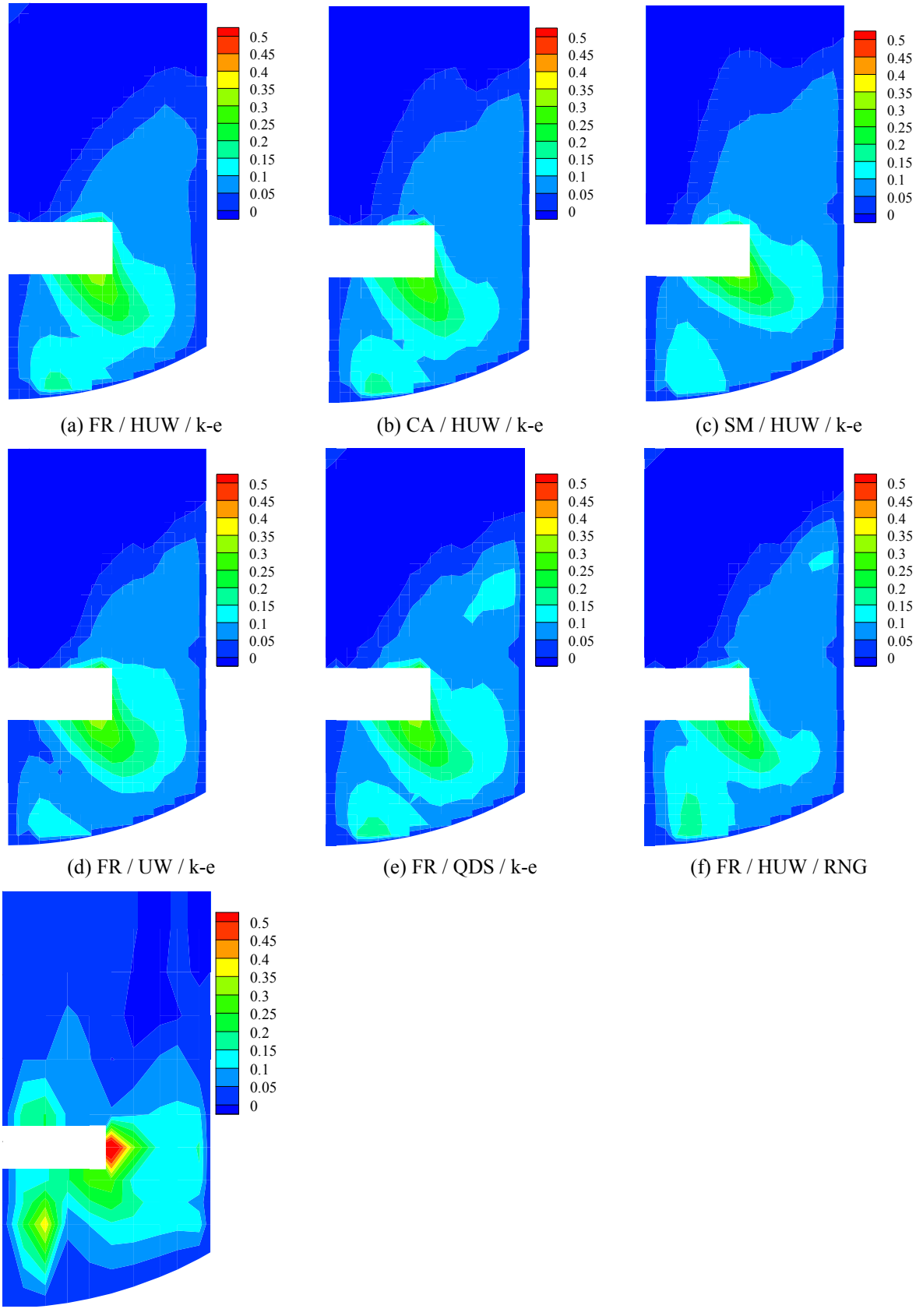

(a) FR / HUW / k-e (b) CA / HUW / k-e (c) SM / HUW / k-e

(d) FR / UW / k-e (e) FR / QDS / k-e (f) FR / HUW / RNG

(g) LDV (Aubin *et al.*, 2001)

Figure 4

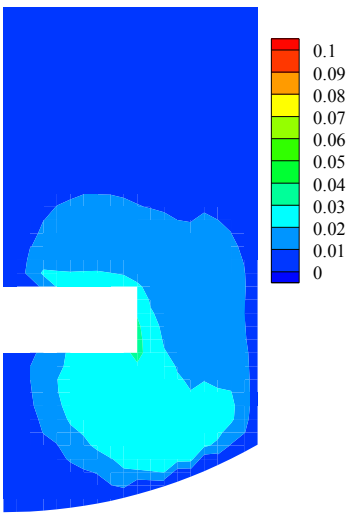

(a) FR / HUW / k-e

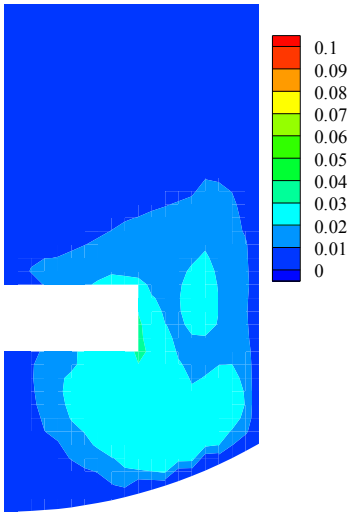

(b) CA / HUW / k-e

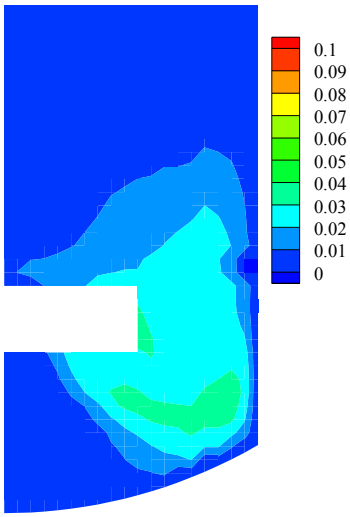

(c) SM / HUW / k-e

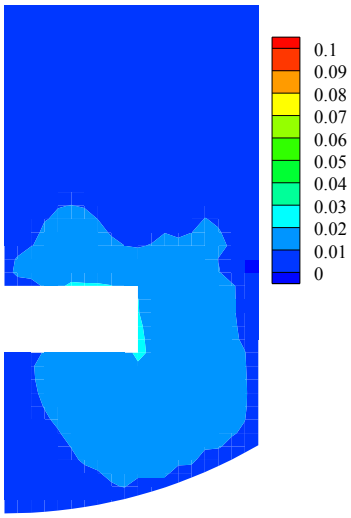

(d) FR / UW / k-e

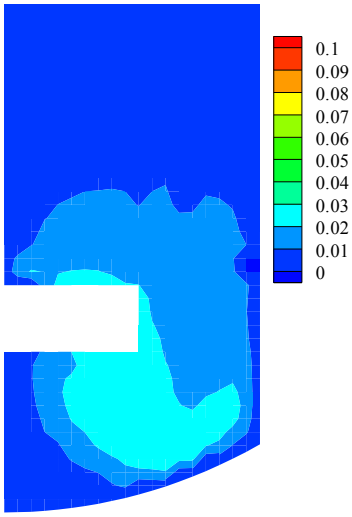

(e) FR / QDS / k-e

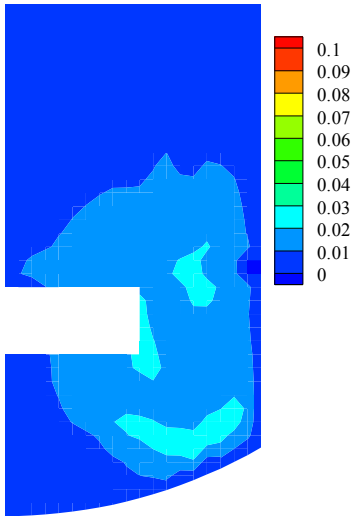

(f) FR / HUW / RNG

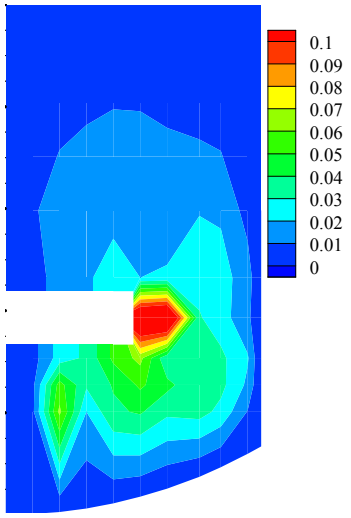

(g) LDV (Aubin *et al*., 2001)

Figure 5

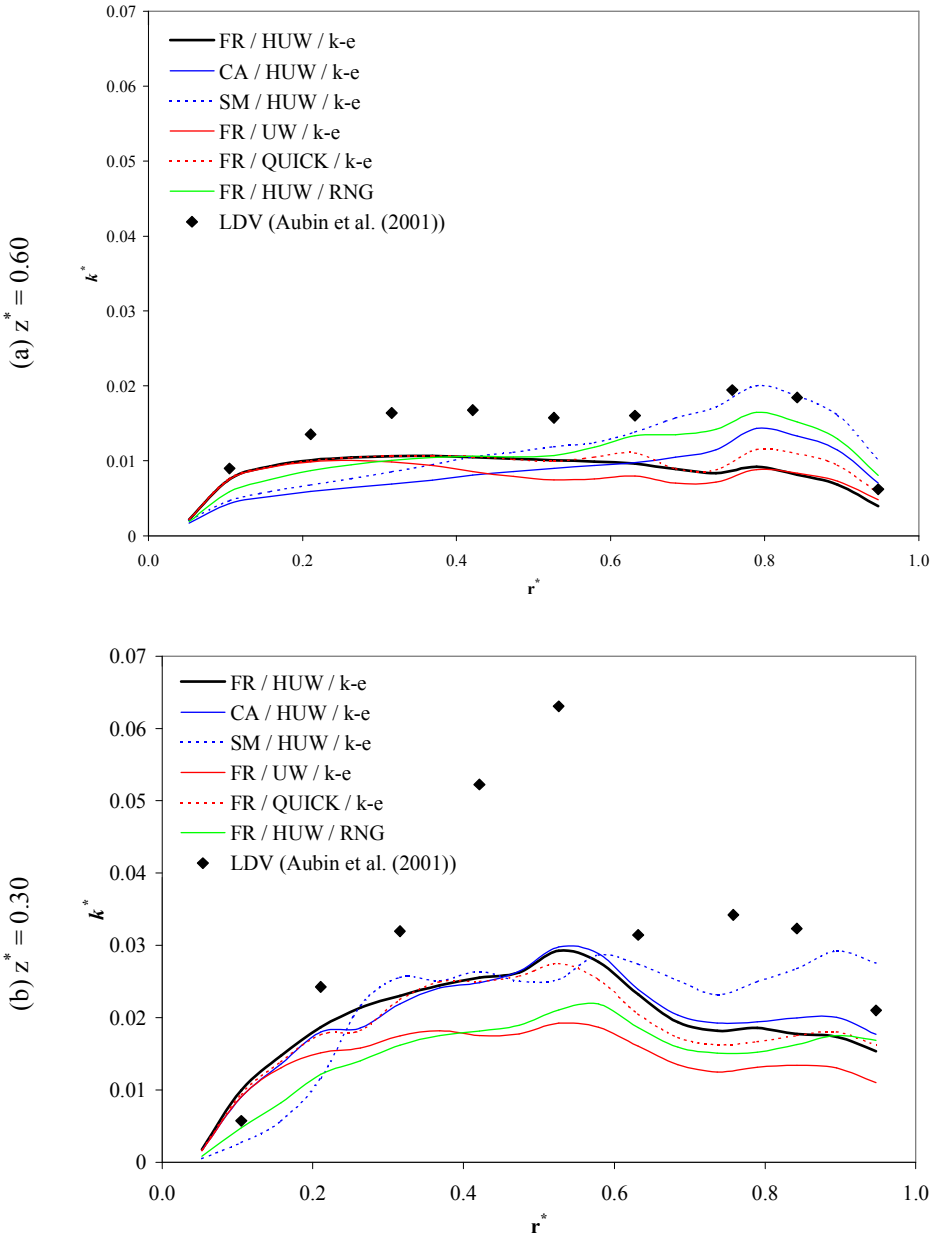
(a) z* = 0.60
FR / HUW / k-e
CA / HUW / k-e
SM / HUW / k-e
FR / UW / k-e
FR / QUICK / k-e
FR / HUW / RNG
LDV (Aubin et al. (2001))
k*
r*
0.07
0.06
0.05
0.04
0.03
0.02
0.01
0
0.0
0.2
0.4
0.6
0.8
1.0
(b) z* = 0.30
FR / HUW / k-e
CA / HUW / k-e
SM / HUW / k-e
FR / UW / k-e
FR / QUICK / k-e
FR / HUW / RNG
LDV (Aubin et al. (2001))
k*
r*

Figure 6

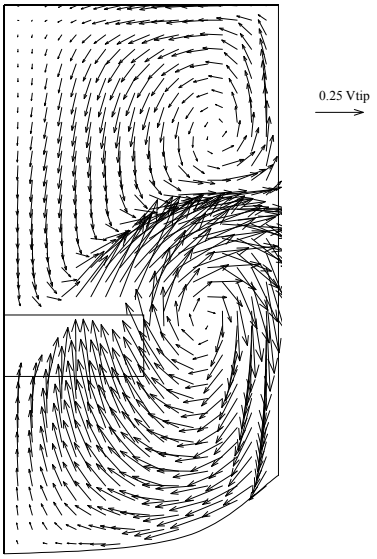

(a) FR / HUW / k-e / UP

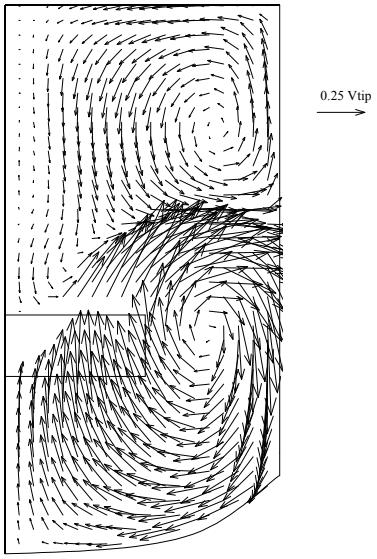

(b) CA / HUW / k-e / UP

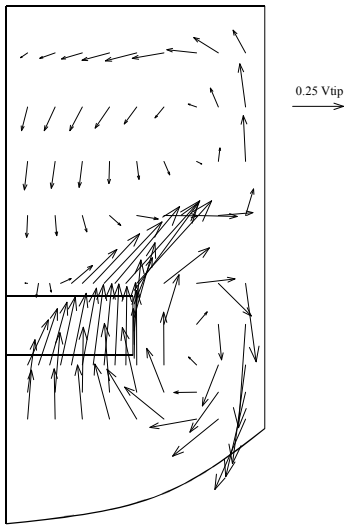

(c) LDV (Aubin *et al*., 2001)

Figure 7

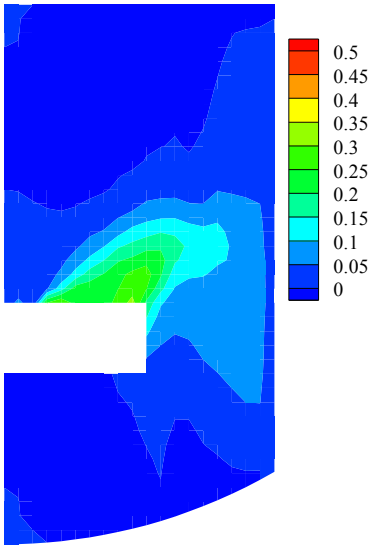

(a) FR / HUW / k-e / UP

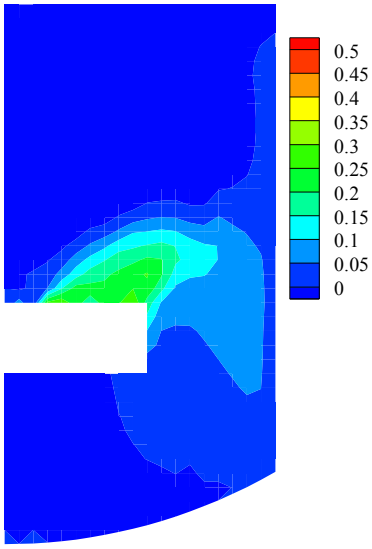

(b) CA / HUW / k-e /UP

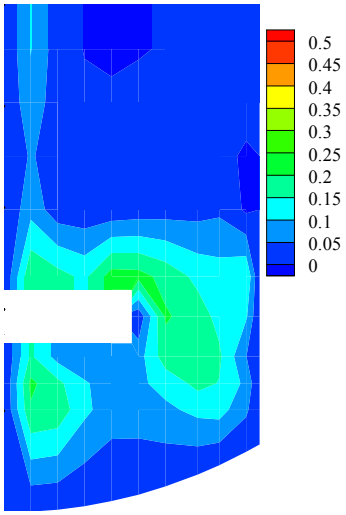

(c) LDV (Aubin *et al*., 2001)

Figure 8

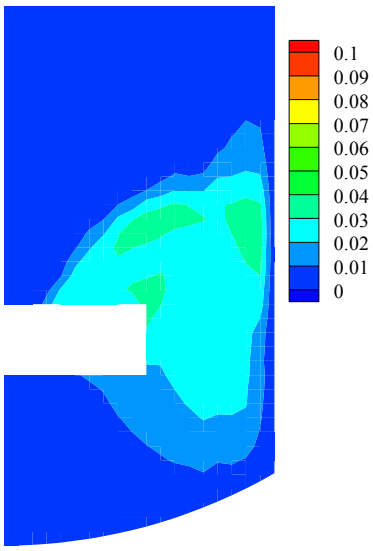

(a) FR / HUW / k-e / UP

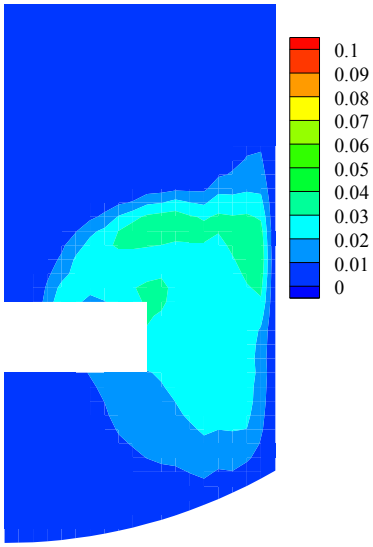

(b) CA / HUW / k-e / UP

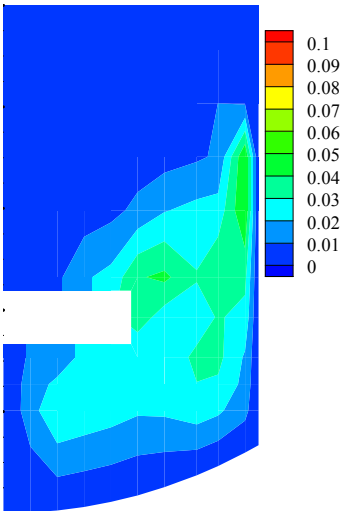

(c) LDV (Aubin *et al*., 2001)

Figure 9

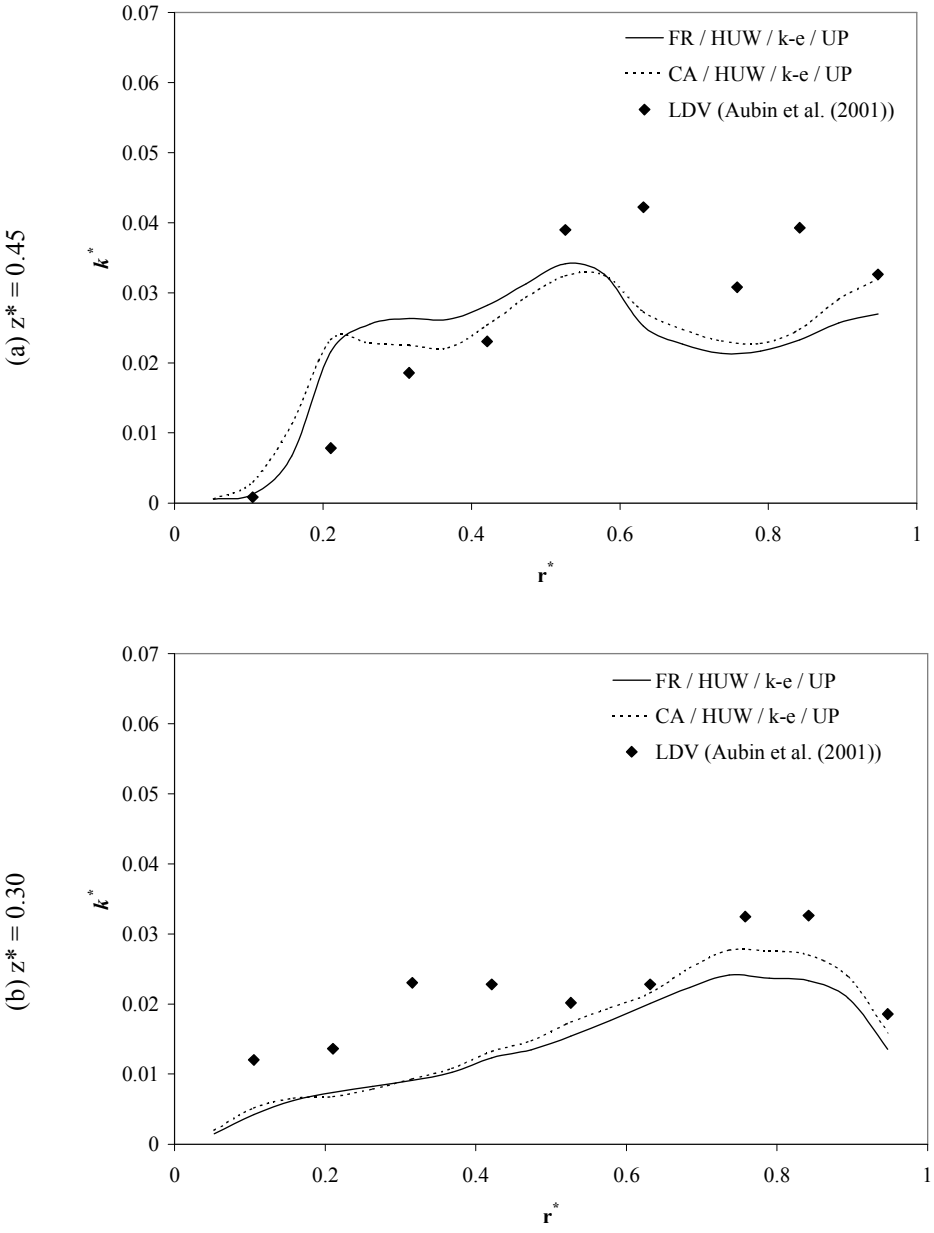
(a) z* = 0.45
FR / HUW / k-e / UP
CA / HUW / k-e / UP
LDV (Aubin et al. (2001))
k*
r*
0.07
0.06
0.05
0.04
0.03
0.02
0.01
0
0.2
0.4
0.6
0.8
1
(b) z* = 0.30
FR / HUW / k-e / UP
CA / HUW / k-e / UP
LDV (Aubin et al. (2001))
k*
r*

Figure 10